

Reorientation of $(\text{Mn}_{\text{Ti}}'' - \text{V}_{\text{O}}^{\bullet})^{\times}$ defect dipoles in acceptor-modified BaTiO_3 single crystals: An electron paramagnetic resonance study

Lixue Zhang,^{1,2} Emre Erdem,^{2,3} Xiaobing Ren,^{4,1} and Rüdiger-A. Eichel^{2,3,a)}

¹State Key Laboratory for Mechanical Behaviour of Materials and Multi-disciplinary Materials Research Center, Xi'an Jiaotong University, Xi'an 710049, People's Republic of China

²Eduard-Zintl-Institut, Technische Universität Darmstadt, Petersenstr. 20, D-64287 Darmstadt, Germany

³Institut für Physikalische Chemie I, Universität Freiburg, Albertstr. 21, D-79104 Freiburg, Germany

⁴Ferroic Physics Group, National Institute for Materials Science, Tsukuba 305-0047, Ibaraki, Japan

(Received 28 July 2008; accepted 30 September 2008; published online 18 November 2008)

The effect of external electric fields on the orientation of $(\text{Mn}_{\text{Ti}}'' - \text{V}_{\text{O}}^{\bullet})^{\times}$ defect dipoles in ferroelectric BaTiO_3 single crystals and its interplay with the domain structure were investigated by means of electron paramagnetic resonance (EPR) spectroscopy and optical microscopy. The results show that in specimens aged in the ferroelectric state for a defined time, so-termed *ferroelectrically aged*, the $(\text{Mn}_{\text{Ti}}'' - \text{V}_{\text{O}}^{\bullet})^{\times}$ defect dipoles orient along the direction of spontaneous polarization and follow the domain switching upon poling with correspondingly high electric fields. A comparison of the EPR signal in poled aged single-domain samples to that in naturally aged multidomain samples indicates a similar reorientation process of the defect dipole, which means that dipole reorientation rather requires long time, thermal energy, and high electric fields, i.e., more energy. © 2008 American Institute of Physics. [DOI: 10.1063/1.3006327]

An important issue in the class of ferroelectric materials is the control and understanding of so-termed *internal bias fields* in order to enhance device reliability. Internal bias fields manifest in voltage shifts of the ferroelectric hysteresis loop and may occur when the device remains in a particular polarization state for a given period of time.^{1–5} Such effects have been proposed arising due to the existence of inherent defect dipoles^{6,7} and their dynamics are being discussed in terms of the *ferroelectric aging* and *imprint failure* phenomena.^{2,8–15}

More generally, such defect dipoles contribute to the overall polarization in a ferroelectric compound, which is comprised of two components—the “bulk” ferroelectric polarization, P_S , and a defect contribution due to an alignment of defect dipoles in the material denoted as P_D .^{6,16–18} Typical defect dipoles include acceptor center—oxygen vacancy associates such as charged $(\text{Fe}'_{\text{Zr,Ti}} - \text{V}_{\text{O}}^{\bullet})^{\bullet}$ (Refs. 19–24) or electrically neutral $(\text{Cu}''_{\text{Zr,Ti}} - \text{V}_{\text{O}}^{\bullet})^{\times}$ (Refs. 25–27) and $(\text{Mn}''_{\text{Ti}} - \text{V}_{\text{O}}^{\bullet})^{\times}$.²⁸

Whereas the fast rearranging processes that take part in domain growth and domain wall motion during poling are quite well understood,³¹ there is currently only a few such detailed information available about the switching dynamics of defect dipoles.^{16–18} In particular, defect dipoles are expected not to switch during fast field cycling^{8–10} because such a process has to involve short-range-order oxygen vacancy diffusion around the acceptor^{29,30} center and consequently has to be considerably slower than the domain switching process and certainly has to involve considerably higher thermal and electric-field energies.

In order to monitor the structure and dynamics of point and extended defects, electron paramagnetic resonance (EPR) (Refs. 32 and 33) assisted by density functional theory^{20,27} has proved being a powerful technique to characterize the defect structure on an atomic scale. For the manganese

functional center in BaTiO_3 the defect structure in terms of an association to charge compensating oxygen vacancies currently is controversially discussed.^{28,34} On the other hand, in BaTiO_3 single crystals the reorientation process of $(\text{Fe}'_{\text{Ti}} - \text{V}_{\text{O}}^{\bullet})^{\bullet}$ defect dipoles has recently been observed by EPR, showing the alignment of defect dipoles along the direction of the spontaneous polarization^{16,17} through an oxygen vacancy motion in the oxygen octahedron about a negatively charged Fe'_{Ti} center.¹⁸ However, simultaneous information on the domain structure that is crucial for the interpretation of the observed results was not available. We therefore aim to extend previous studies on the switching behavior of defect dipoles by simultaneously monitoring the domain configuration via optical microscopy. Moreover, we compared the EPR signals in poled aged single-domain BaTiO_3 crystals with that in ferroelectrically aged multidomain specimen in order to gain more insights into the interplay between internal field and aging process.

The investigated sample here is a manganese doped barium titanate single crystal that is grown from a BaCl_2 flux at 1300 °C under argon atmosphere. The *c*-axis of the single crystal was proven to be along the thickness direction. The EPR measurements were performed on an X-band (9.4 GHz) Bruker ESP 380 spectrometer with an H_{011} cavity.

For a theoretical description of the obtained EPR spectra the spin-Hamiltonian concept is used.³⁵ The free divalent manganese ion has a $3d^5$ electronic configuration and its ground state is ${}^5S_{5/2}$ with $S = \frac{5}{2}$, resulting in the following spin-Hamiltonian

$$\mathcal{H} = \beta_e \mathbf{B}_0 \cdot \mathbf{g} \cdot \mathbf{S} + \sum_{k=2, \dots, 4}^{k \leq q \leq k} B_k^q O_k^q(S_x, S_y, S_z) + \mathbf{S} \cdot {}^{55}\mathbf{A} \cdot \mathbf{I}, \quad (1)$$

where β_e denotes the Bohr magneton, \mathbf{B}_0 is the external magnetic field, \mathbf{g} is the electron \mathbf{g} -matrix, B_k^q are the fine-structure (FS) Hamiltonian coefficients, and O_k^q are the extended Stevens spin operators.³⁵ The first term represents the elec-

^{a)}FAX: +49-761-2036222. Electronic mail: r.eichel@physchem.uni-freiburg.de.

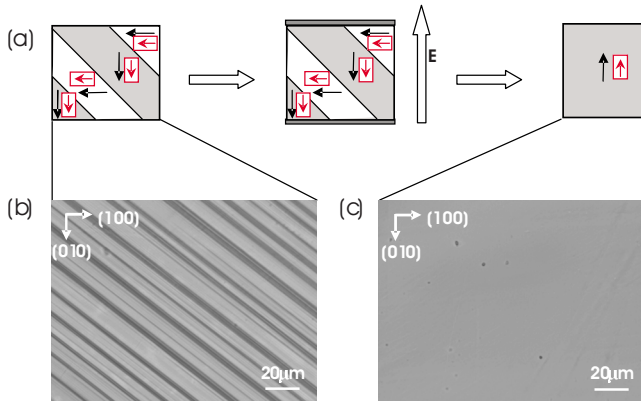


FIG. 1. (Color online) (a) Schematic of the poling process involving arrows for the spontaneous polarization (black) and the defect polarization (red). [(b) and (c)] Optical microscope images showing the domain configuration in the (b) initial multidomain and (c) poled single-domain states.

tronic Zeeman interaction and the second term is the effective FS Hamiltonian, describing the interaction of the crystal field with the paramagnetic ion. The order k in the spin operators is restricted by $k \leq 2S$ and $q \leq k$, allowing terms up to $k=4$ for $S=\frac{5}{2}$. The last term describes the manganese hyperfine interaction owing to the interaction with 100% natural abundance ^{55}Mn -isotope with $I=\frac{5}{2}$, where ^{55}A is the corresponding hyperfine-interaction tensor. Typically, for S -state ions, considerable simplifications through the use of isotropic g_{iso} -values and hyperfine-coupling constants $^{55}a_{\text{iso}}$ are justified, which render the following simplified spin-Hamiltonian

$$\mathcal{H} = g_{\text{iso}}\beta_e\mathbf{B}_0 \cdot \mathbf{S} + \sum_{k=2,\dots,4}^{-k \leq q \leq k} B_k^q O_k^q(S_x, S_y, S_z) + ^{55}a_{\text{iso}}\mathbf{S} \cdot \mathbf{I}. \quad (2)$$

At ambient temperature, the initial state of the crystal may be described by a *multidomain* configuration [Fig. 1(b)].

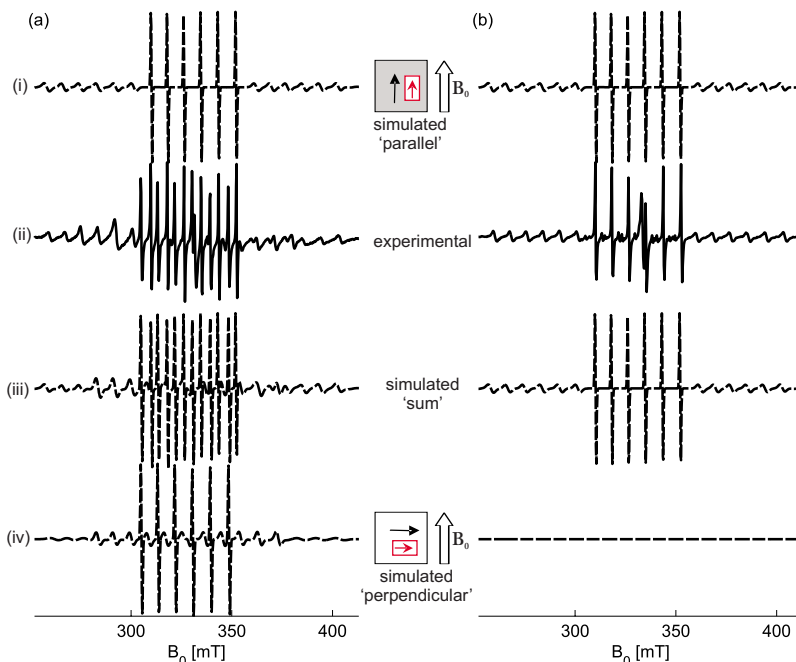


FIG. 2. (Color online) X-band (9.4 GHz) EPR spectra of the $(\text{Mn}_{\text{Ti}}^{\text{II}}-\text{V}_{\text{O}}^{\text{**}})^{\times}$ defect dipole center in a BaTiO_3 single crystal. (a) Initial multidomain state. (b) Poled single-domain state after a treatment of 1.5 kV/mm (250 V) at a temperature of 40 °C for 4 h. The experimental spectra [(ii), bold] are compared with numerical spectrum simulations (iii, dashed). For the initial multidomain state (a) the spectrum is a superposition of two magnetically equivalent centers of different orientations [(i) and (iv)]; one being oriented parallel to the external magnetic field (i) and the other in perpendicular (iv). After poling (b) the single-domain state only consists of a center oriented parallel to the external magnetic field (iv).

Thereafter, the sample was “aged” at room temperature for a long time. The corresponding EPR spectrum of the aged multidomain sample is shown in Fig. 2(a)(ii). The spectrum is dominated by two sets of sextet ^{55}Mn -hyperfine multiplets of the central $|m_S=-\frac{1}{2}\rangle \leftrightarrow |+\frac{1}{2}\rangle$ transition and less intense sextets of the higher $|m_S=\mp\frac{5}{2}, \frac{3}{2}\rangle \leftrightarrow |+\frac{3}{2}, \frac{1}{2}\rangle$ transitions. By numerical spectrum simulation,³⁶ the experimental spectrum may be reproduced by means of two magnetically equivalent centers of axial site symmetry ($B_2^0=240$ MHz and $B_2^2=0$) but different orientation with respect to the external magnetic field in the EPR experiment. The corresponding numerically simulated spectrum [Fig. 2(a)(iii)] consequently is a sum of two individual subspectra that are obtained by assuming an identical set of spin-Hamiltonian parameters but different orientations [Figs. 2(a)(i) and 2(a)(iv)].

The observation corresponds to $(\text{Mn}_{\text{Ti}}^{\text{II}}-\text{V}_{\text{O}}^{\text{**}})_{\parallel}^{\times}$ defect dipoles oriented along the direction of P_S (along the crystallographic c -axis). Owing to the observed multidomain state, the defect dipoles are once oriented along the direction of the external magnetic field and once perpendicular to it. Based on the values of the electronic g -value ($g_{\text{iso}}=2.003$) and the size of the hyperfine splitting ($^{55}a_{\text{iso}}=237$ MHz), the charge state of the manganese functional center is found being divalent, which corresponds to an acceptor-type center. The refined spin-Hamiltonian values are perfectly consistent with earlier reported values.^{28,34,37-41}

As expected for a well-aged sample⁸ within the domains, the majority of defect dipoles is oriented along the direction of spontaneous polarization $(\text{Mn}_{\text{Ti}}^{\text{II}}-\text{V}_{\text{O}}^{\text{**}})_{\parallel}^{\times}$. No signature from dipoles perpendicular to this orientation $(\text{Mn}_{\text{Ti}}^{\text{II}}-\text{V}_{\text{O}}^{\text{**}})_{\perp}^{\times}$ could be observed within the EPR detection limit of approximately 10^{11} spins,⁴² assuming a signal-to-noise ratio of unity. This observation is in contrast to the earlier reported results on $(\text{Fe}_{\text{Ti}}^{\text{II}}-\text{V}_{\text{O}}^{\text{**}})^{\times}$ in BaTiO_3 single crystals that assume an equal distribution of orientations for the defect dipoles along and perpendicular to the direction of spontaneous polarization.^{16,17} However, an orientation perpendicular to P_S and thus perpendicular to the crystallographic c -axis would result in a site symmetry for the $(\text{Fe}_{\text{Ti}}^{\text{II}}-\text{V}_{\text{O}}^{\text{**}})^{\times}$ center that is

lower than axial ($B_2^2 \neq 0$), which is in contrast to the EPR spectra shown^{16,17} and also to the results reported in this letter. Hence, the varying intensities for the different dipoles parallel and perpendicular to the direction of the magnetic field have rather to be interpreted in terms of the existing domain structure.

An important consequence of the axiality of the determined FS-interaction tensor is that the $(\text{Mn}_{\text{Ti}}'' - \text{V}_{\text{O}}^{\bullet\bullet})_{\parallel}^{\times}$ defect dipoles impact the direction of polarization in the neighboring unit cells. This phenomenon may be explained by the ferroelectric aging phenomenon on the basis of the symmetry-conforming short-range-ordering principle,^{8–11,13} after which during aging the defect dipoles follow the orientation of P_S in the ferroelectric state. Furthermore, no (detectable) fraction of the $(\text{Mn}_{\text{Ti}}'' - \text{V}_{\text{O}}^{\bullet\bullet})_{\parallel}^{\times}$ defect dipoles is found at a domain wall; clearly for such a situation an additional center with local site symmetry lower than axial would be expected.

Subsequent to the characterization of the initial unpoled state, we applied an electric field of 1.5 kV/mm (250 V) to the sample along its thickness direction at a temperature of 40 °C for 4 h. The sample was thus transformed into a *single-domain* state after this poling process [Fig. 1(c)]. Before the EPR measurement, the specimen was aged at the same temperature for 40 h. The corresponding EPR results are depicted in Fig. 2(b)(ii). The spectrum now may be described in terms of a single center [Fig. 2(b)(i)]; the spin-Hamiltonian parameters have not changed. Consequently, the contribution of the second center to the simulated sum spectrum vanishes [Fig. 2(b)(iv)]. This indicates that all $(\text{Mn}_{\text{Ti}}'' - \text{V}_{\text{O}}^{\bullet\bullet})_{\parallel}^{\times}$ defect dipoles are now aligned along the same direction, namely, the direction of spontaneous polarization. Furthermore, this defect-dipole alignment induced by an external field is similar to that for ferroelectric aging in a multidomain sample. Thus, information about the external fields during poling will be most helpful to quantitatively understand the interplay between internal fields developed after the ferroelectric aging process.

Consequently, the $(\text{Mn}_{\text{Ti}}'' - \text{V}_{\text{O}}^{\bullet\bullet})_{\parallel}^{\times}$ defect dipoles were re-oriented along the direction of the applied electric field after a poling treatment of 1.5 kV/mm (250 V) at a temperature of 40 °C for 4 h. This indicates that defect dipoles will not reorient during fast field cycling^{8–10} but rather require long time, high thermal energy, and high electric fields. Obviously, future activities will focus on the kinetics of the reported switching process here.

The authors are very grateful to Professor Dr. Rolf Böttcher and Dipl.-Ing. Joachim Höntsch for continuous support and many fruitful discussions. This research has been financially supported by the DFG Center of Excellence 595 “Electrical Fatigue in Functional Materials” and National Science Foundation of China (Grant No. 50702042).

- ¹H.-J. Hagemann, *J. Phys. C* **11**, 3333 (1978).
- ²G. Arlt and H. Neumann, *Ferroelectrics* **87**, 109 (1988).
- ³A. Schulze and K. Ogino, *Ferroelectrics* **87**, 361 (1988).
- ⁴D. A. Hall and P. J. Stevenson, *Ferroelectrics* **187**, 23 (1996).
- ⁵D. A. Hall, M. M. Ben-Omran, and P. J. Stevenson, *J. Phys.: Condens. Matter* **10**, 461 (1998).
- ⁶P. V. Lambeck and G. H. Jonker, *Ferroelectrics* **22**, 729 (1978).
- ⁷P. V. Lambeck and G. H. Jonker, *J. Phys. Chem. Solids* **47**, 453 (1986).
- ⁸X. Ren, *Nature Mater.* **3**, 91 (2004).
- ⁹L. X. Zhang, W. Chen, and X. Ren, *Appl. Phys. Lett.* **85**, 5658 (2004).
- ¹⁰L. X. Zhang and X. Ren, *Phys. Rev. B* **71**, 174108 (2005).
- ¹¹L. X. Zhang and X. Ren, *Phys. Rev. B* **73**, 094121 (2006).
- ¹²M. M. Ahmada, K. Yamada, P. Meuffels, and R. Waser, *Appl. Phys. Lett.* **90**, 112902 (2007).
- ¹³H. Bao, L. X. Zhang, Y. Wang, W. F. Liu, C. Zhou, and X. Ren, *Appl. Phys. Lett.* **91**, 142903 (2007).
- ¹⁴D. A. Hall and M. M. Ben-Omran, *J. Phys.: Condens. Matter* **10**, 9129 (1998).
- ¹⁵W. L. Warren, D. Dimos, G. E. Pike, K. Vanheusden, and R. Ramesh, *Appl. Phys. Lett.* **67**, 1689 (1995).
- ¹⁶D. C. Lupascu, *Fatigue in ferroelectric ceramics and related issues* (Springer, Heidelberg, 2004).
- ¹⁷W. L. Warren, G. E. Pike, K. Vanheusden, D. Dimos, B. A. Tuttle, and J. Robertson, *J. Appl. Phys.* **79**, 9250 (1996).
- ¹⁸W. L. Warren, K. Vanheusden, D. Dimos, G. E. Pike, and B. A. Tuttle, *J. Am. Ceram. Soc.* **79**, 536 (1996).
- ¹⁹H. Meštrić, R.-A. Eichel, K.-P. Dinse, A. Ozarowski, J. van Tol, and L. C. Brunel, *J. Appl. Phys.* **96**, 7440 (2004).
- ²⁰H. Meštrić, R.-A. Eichel, T. Kloss, K.-P. Dinse, So. Laubach, St. Laubach, and P. C. Schmidt, *Phys. Rev. B* **71**, 134109 (2005).
- ²¹H. Meštrić, R.-A. Eichel, K.-P. Dinse, A. Ozarowski, J. van Tol, L. C. Brunel, H. Kungl, M. J. Hoffmann, K. A. Schönau, M. Knapp, and H. Fuess, *Phys. Rev. B* **73**, 184105 (2006).
- ²²E. Erdem, R.-A. Eichel, H. Kungl, M. J. Hoffmann, A. Ozarowski, H. van Tol, and L. C. Brunel, *Phys. Scr., T* **129**, 12 (2007).
- ²³E. Erdem, R.-A. Eichel, H. Kungl, M. J. Hoffmann, A. Ozarowski, H. van Tol, and L. C. Brunel, *IEEE Trans. Ultrason. Ferroelectr. Freq. Control* **55**, 1061 (2008).
- ²⁴E. Erdem, M. D. Drahus, R.-A. Eichel, H. Kungl, M. J. Hoffmann, A. Ozarowski, H. van Tol, and L. C. Brunel, *Funct. Mat. Lett.* **1**, 7 (2008).
- ²⁵R.-A. Eichel, H. Kungl, and M. J. Hoffmann, *J. Appl. Phys.* **95**, 8092 (2004).
- ²⁶R.-A. Eichel, P. Erhart, P. Träskelin, K. Albe, H. Kungl, and M. J. Hoffmann, *Phys. Rev. Lett.* **100**, 095504 (2008).
- ²⁷P. Erhart, R.-A. Eichel, P. Träskelin, and K. Albe, *Phys. Rev. B* **76**, 174116 (2007).
- ²⁸R.-A. Eichel and R. Böttcher, *Mol. Phys.* **105**, 2195 (2007).
- ²⁹M. S. Islam, *J. Mater. Chem.* **10**, 1027 (2000).
- ³⁰M. S. Islam, *Solid State Ionics*, **154–155**, 75 (2002).
- ³¹D. Damjanovic, *The Science of Hysteresis*, edited by I. Mayergoyz and G. Bertotti (Elsevier, Oxford, 2005), pp. 337–465.
- ³²R.-A. Eichel, *J. Electroceram.* **19**, 9 (2007).
- ³³R.-A. Eichel, *J. Am. Ceram. Soc.* **91**, 691 (2008).
- ³⁴R. Böttcher, C. Klimm, D. Michel, H.-C. Semmelhack, G. Völkel, H.-J. Gläsel, and E. Hartmann, *Phys. Rev. B* **62**, 2085 (2000).
- ³⁵A. Abragam and B. Bleaney, *Electron Paramagnetic Resonance of Transition Ions* (Clarendon, Oxford, 1970).
- ³⁶S. Stoll and A. Schweiger, *J. Magn. Reson.* **178**, 42 (2006).
- ³⁷H. Ikushima, *J. Phys. Soc. Jpn.* **21**, 1866 (1966).
- ³⁸H. Ikushima, *J. Phys. Soc. Jpn.* **23**, 540 (1967).
- ³⁹E. Siegel and K. A. Müller, *Phys. Rev. B* **19**, 109 (1979).
- ⁴⁰K. A. Müller, W. Berlinger, K. W. Blazey, and J. Albers, *Solid State Commun.* **61**, 21 (1987).
- ⁴¹B. Milsch, *Phys. Status Solidi A* **133**, 455 (1992).
- ⁴²G. Feher, *Bell Syst. Tech. J.* **36**, 449 (1957).